Evaluation of scleral-fixated intraocular lens position anomalies by anterior segment optical coherence tomography

Nihat POLAT[1,]*, Kemalettin Kazım DEVRANOĞLU[2], Mehmet Akif ÖZDAMAR[3], Ceyhun ARICI[3]

[1]Department of Ophthalmology, Faculty of Medicine, İnönü University, Malatya, Turkey
[2]Dünya Eye Hospital, İstanbul, Turkey
[3]Department of Ophthalmology, Cerrahpaşa Medical Faculty, İstanbul University, İstanbul, Turkey

Background/aim: To measure the positions of scleral-fixated intraocular lenses (IOLs) using anterior segment optical coherence tomography (OCT) and to evaluate the influence of the position of scleral-fixated IOL on the quality of vision.

Materials and methods: Twenty-six eyes of 26 patients were included in the study. The average age was 57.5 (11 to 78) years. Anterior segment images were taken using slit lamp optical coherence tomography (SL-OCT) and were used to evaluate the position of the IOL.

Results: The average amounts of tilt and decentration were 2.25° ± 1.93° and 359.28 ± 194.70 µm, respectively. There was a positive and moderate relationship between tilt and astigmatism caused by the position of the IOL (P = 0.030). No relationship was detected between decentration and the astigmatism caused by the position of the IOL (P = 0.285).

Conclusion: Scleral-fixated IOL position can be evaluated with SL-OCT, which is a noncontact, noninvasive, reproducible, and reliable method of evaluation. Anterior segment OCT has been shown to provide sensitive measurements but not in all cases. The present study showed that a tilted scleral-fixated IOL behaved like a toric IOL, and the astigmatism caused by the position of the scleral-fixated IOL therefore could increase or decrease total astigmatism.

Key words: Cataract, intraocular lens position, optical coherence tomography, scleral-fixated lens

1. Introduction

The position of the intraocular lens (IOL) has a profound influence on the success of visual rehabilitation and the quality of vision. Scleral-fixated IOL implantation surgery has been performed for a long time, and the associated techniques are well known. However, it is still not always possible to ideally position the implanted lens (1,2).

The factors that lead to position abnormalities include the inability of the IOL haptic flaps to be placed 180° from each other, suturing errors, failure to pass the sutures through the relevant region when entering through the sclera, failure to correctly place the haptics in the ciliary sulcus, and haptic breakage (3). Such position abnormalities cause optical aberrations (4). These position abnormalities can be examined with biomicroscopy, ultrasonic biomicroscopy, Scheimpflug video photography and optical coherence tomography (OCT). OCT is a noninvasive, noncontact, sensitive, and reproducible technique (5,6).

Our aim in the present study was to measure the positions of scleral-fixated IOLs using OCT as a new method. We also aimed to evaluate the influence of the position of the scleral-fixated IOLs on the quality of vision of patients who had undergone scleral-fixated IOL implantation surgery.

2. Materials and methods

In total, 26 eyes of 26 patients (14 women, 12 men) who had undergone scleral-fixated IOL implantation surgery to correct aphakia at the Department of Ophthalmology of the Cerrahpaşa Faculty of Medicine at İstanbul University were included in the retrospective study. All of the surgeries had been conducted by the same surgeon. The mean age of the patients was 57.5 years and the age range was 11 to 78 years. Informed consent was obtained from each patient included in the study.

Information regarding the demographics and medical history of each patient including age, sex, cause of aphakia, corneal incision type, and scleral-fixated implanted IOL type were recorded.

2.1. Study exclusion criteria

Patients whose ocular media were not transparent (due to corneal opacity, corneal edema, vitreous hemorrhage, vitritis, or endophthalmitis), those who presented with ocular pathology (such as retinal detachment, macular diseases, optic disc anomalies, optic disc edema, glaucoma, and uveitis), and patients whose pupils did not sufficiently dilate were excluded from the study due to the potential for inaccuracies in their OCT measurements.

2.2. Methods

The visual acuity of each patient included in the study was determined with and without correction using the Snellen chart, and refractive errors were determined using a Topcon KR-8800 autorefractometer (Topcon Corporation, Tokyo, Japan). All participants had undergone scleral-fixated intraocular lens (IOL) implantation surgery at least 1 year prior to participating in the study. Their intraocular pressures were measured with a Topcon CT80 noncontact tonometer (Topcon Corporation, Tokyo, Japan). Detailed biomicroscopy and fundus examinations were performed. A Keratron Scout videokeratoscope (Optikon 2000 Industrie, Rome, Italy) was used to assess the corneal topography of each patient. The simK1 and simK2 corneal topography measurements were repeated 3 times each to determine an average value for each. The measurements obtained from the topographic maps were recorded for further evaluation in the study.

A slit lamp optical coherence tomography device (SL-OCT) (Heidelberg Engineering Gmbh, Dossenheim, Germany) was used to evaluate the position of the intraocular lens. Five horizontal sections were obtained from horizontal screenings along a 0°–180° axis while the patient's eye was focused on the fixation point. The image that produced the highest resolution of the corneal–scleral and lens contours was used for the image analysis.

The best OCT images of the anterior segment were selected for further analysis and were transferred into ImageJ (http://rsb.info.nih.gov/ij/) (Figure 1).
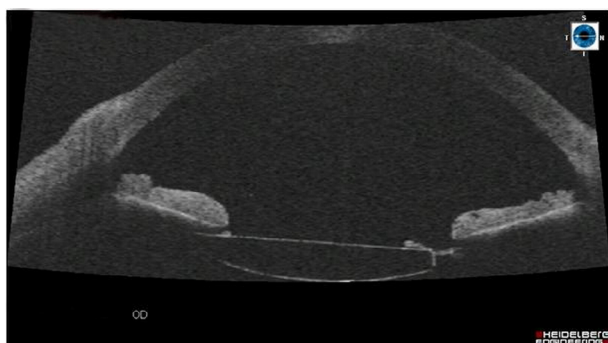
The 3-point circular region of interest (ROI) tool in ImageJ was used to determine the reference points (A and B) for the iridocorneal angles in the ocular image, and the horizontal axis of the eye (X_1) was then drawn along the line connecting these 2 points. The optical axis of the eye (Y_1), which passes through the centers of the horizontal axis and the corneal vertex of the eye and intersects the horizontal axis at an angle of 90°, was also drawn (Figure 2).
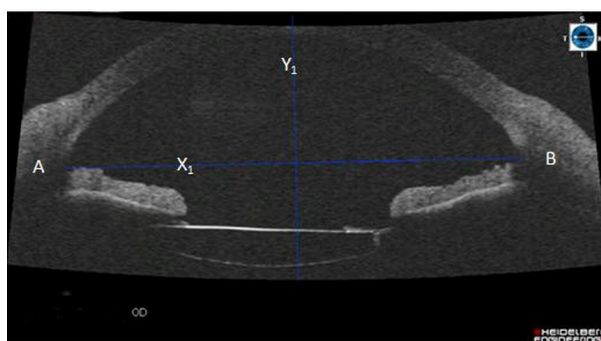
The anterior and posterior lines, which depict the curvatures of the anterior and posterior surfaces of the lens, were drawn by marking 3 separate points (C, D, and E) along the anterior line of each lens image and an additional 3 separate points (F, G, and H) along the posterior line of each lens image (Figure 3).

The horizontal axis (X_2) of the lens was determined by drawing a line that passed through the 2 intersections of the anterior and posterior curvature lines. The vertical axis of the lens, which passes through the center of the horizontal axis of the lens and intersects the horizontal axis of the lens at an angle of 90°, was also drawn (Figure 4).

The distance between the optical axis of the eye (Y_1) and the center of the horizontal axis of the lens (X_2) was calculated using ImageJ, and the level of decentration was determined using this distance. The angle between the optical axis of the eye (Y_1) and the vertical axis of the lens (Y_2) was also calculated using ImageJ and was used to determine the tilt angle.

2.3. Statistical analysis

SPSS 13.0 for Windows (Chicago, IL, USA) was used for statistical analysis. The numerical variables all included mean, standard deviation, median, minimum, and maximum values. The Shapiro–Wilk test was used for normality tests. Spearman's correlation coefficient was used to evaluate relationships between nonparametric variables. $P < 0.05$ was assumed to signify statistical significance for all statistical analyses.

Figure 1. OCT image from the anterior segment of a case (the decentralization of the IOL to the left side of the figure).

Figure 2. Drawing of the ocular axes in an image from the same case presented in Figure 1 using the 3-point circular ROI application in ImageJ.
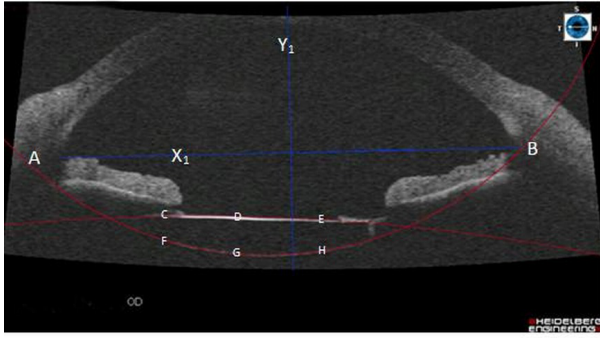
Figure 3. Drawing of the anterior and posterior curvature lines of the lens in an image from the same case presented in the previous figures.
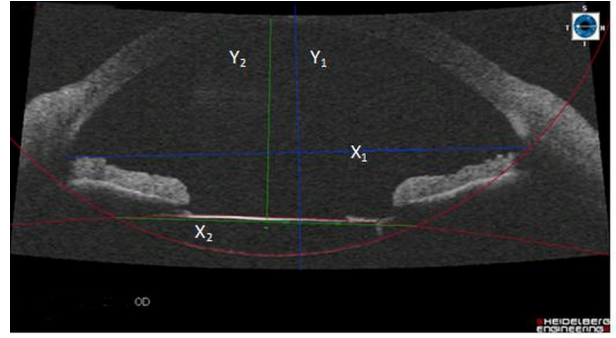
Figure 4. Drawing of the lens axes in an image from the same case presented in the previous figures.

3. Results

Eight patients were excluded from the statistical analysis due to unclear lens images in anterior segment views. The values for tilt and decentration, degrees of astigmatism, and visual acuities of the patients who participated in the study are presented in Table 1 while the numerical variables are given with mean, standard deviation, median, minimum, and maximum values in Table 2.

The mean tilt and decentration values were 2.25° ± 1.93° and 359.28 ± 194.70 μm, respectively. The average amount of astigmatism by position of the intraocular lens was 0.635 ± 0.628 μm.

Correlation assessments revealed a positive and moderate relationship between tilt and astigmatism caused by the position of the IOL, with P = 0.030. On the other hand, no relationship was detected between

Table 1. Tilt, decentration, astigmatism, and visual acuity values for each patient. D = diopter.

Patient	Tilt (°)	Decentration (μm)	Corneal astigmatism (D)	Astigmatism caused by position of the IOL (D)	Total astigmatism (D)	Uncorrected visual acuity	Corrected visual acuity
1	1.0	150	2.00	0.75	1.25	0.6	0.85
2	1.0	440	1.80	0.05	1.75	0.3	0.6
3	1.0	190	2.80	0.55	2.25	0.2	0.7
4	1.5	430	0.07	1.82	1.75	0.1	0.7
5	2.5	860	3.10	1.35	1.75	0.2	0.8
6	6.0	268	8.50	0.50	8.00	0.1	0.45
7	6.0	235	1.80	2.20	4.00	0.3	1.0
8	1.0	430	1.20	0.20	1.00	0.2	0.8
9	0.5	430	1.90	0.15	1.75	0.4	0.9
10	0.5	0	1.40	0.40	1.00	0.6	1.0
11	1.3	440	1.90	0.85	2.75	0.5	1.0
12	2.1	225	1.00	2.25	3.25	0.3	0.9
13	1.3	265	3.70	0.45	3.25	0.5	1.0
14	5.0	540	2.50	0.50	2.00	0.4	0.85
15	5.0	335	1.10	0.65	1.75	0.6	1.0
16.	2.5	219	4.20	0.95	3.25	0.35	1.0
17	–	–	3.30	0.20	3.50	0.6	0.9
18	–	–	2.50	0.75	3.25	0.4	0.8
19	–	–	2.70	0.20	2.50	0.4	0.7
20	–	–	3.90	0.35	4.25	0.3	0.8
21	–	–	2.30	0.20	2.50	0.1	0.5
22	–	–	2.60	0.15	2.75	0.35	0.9
23	–	–	1.70	0.80	2.50	0.4	0.8
24	–	–	1.60	0.10	1.50	0.2	0.6
25	0	410	1.10	0.10	1.00	0.5	0.8
26	2.30	600	1.30	0.05	1.25	0.35	0.75

Table 2. Numerical variables.

	n		
Tilt	18	Mean ± SD	2.25 ± 1.93
		Median (min–max)	1.40 (0–6)
Decentration	18	Mean ± SD	359.28 ± 194.70
		Median (min–max)	372.50 (0–860)
Astigmatism caused by position of the IOL	26	Mean ± SD	0.635 ± 0.628
		Median (min–max)	0.475 (0.05–2.25)
Corneal astigmatism	26	Mean ± SD	2.384 ± 1.587
		Median (min–max)	0.475 (0.07–8.50)
Uncorrected visual acuity	26	Mean ± SD	0.356 ± 0.157
		Median (min–max)	0.35 (0.10–0.60)
Corrected visual acuity	26	Mean ± SD	0.811 ± 0.156
		Median (min–max)	0.80 (0.45–1.00)

tilt and uncorrected or corrected visual acuity, with P = 0.214 and P = 0.763, respectively. No relationship was detected between decentration and astigmatism caused by the position of the IOL or uncorrected visual acuity or corrected visual acuity, with P = 0.285, P = 0.326, and P = 0.169, respectively.

The largest tilt angle and decentration distance measured were 6° and 860 μm, respectively. The levels of astigmatism in the 2 patients who exhibited the largest tilt angle (6°) were quite high (4.00 and 8.00 diopters (D)). Patients who had high degrees of tilt in the positioning of their IOLs also had relatively poor uncorrected visual acuities, but no statistically significant correlation was found between tilt value and visual acuity.

4. Discussion
Proper positioning and on-axis alignment of the intraocular lens (IOL) are critical for obtaining satisfactory quality of vision after cataract surgery. Patients with tilted or decentered IOLs may be unhappy with the results of an otherwise successful procedure. In fact, malposition of an IOL is one of the leading indications for removal, exchange, or repositioning of a posterior chamber IOL (7–11).

Significant levels of tilt and decentration can occur following scleral-fixated IOL implantation surgery performed in the absence of capsular support (12,13). These position anomalies cause visual symptoms, but the level of tilt and/or decentration required to induce visual symptoms remains uncertain (14). Tilt or decentration in an IOL induces irregular astigmatism, coma, and spherical aberrations. Consequently, patients with IOL position anomalies complain of visual symptoms such as glare and halo (15).

The present study showed that a tilted scleral-fixated IOL behaved like a toric IOL, and the astigmatism caused by the position of the scleral-fixated IOL therefore could increase or decrease total astigmatism.

Using ultrasonic biomicroscopy, Steiner et al. (16) showed that the haptics of a scleral-fixated IOL were found in the ciliary sulcus only 33% of the time. In another study, performed with gonioscopy, Holland et al. (17) found that 77% of the haptics were located in the ciliary sulcus while 23% of them had relocated posteriorly following scleral-fixated IOL surgery.

Durak et al. (18) reported a mean tilt and decentration of 6.09° ± 3.80° and 0.67 ± 0.43 mm, respectively, for transsclerally sutured posterior chamber IOLs.

Tilt and decentration have also been shown to cause myopic changes, oblique astigmatism, and lateral focus shifts (19). The proper centration of an IOL depends on the symmetry and positional stability of its haptics (20). The recently developed scleral fixation techniques for surgical IOL implantation cannot ensure that the haptics will be located in the ciliary sulcus (21).

Hayashi et al. (22) used Scheimpflug video photography to obtain quantitative measurements of the levels of tilt and decentration in patients who had undergone scleral-fixated IOL implantation. They reported a mean tilt angle of 6.35° ± 3.09° and a decentration of 0.62 ± 0.31 mm in eyes with a scleral suture-fixed IOLs, which were significantly greater than the values obtained in eyes with in-the-bag IOLs showing a tilt angle of 3.18° ± 1.66° and decentration length of 0.29 ± 0.21 mm.

Oshika et al. (23) also used Scheimpflug video photography to assess the average tilt angle and decentration in patients who had undergone scleral-fixated IOL implantation. They found that the mean tilt

angle and decentration distance were 4.43° and 0.28 mm, respectively.

In the present study, the average values for tilt and decentration obtained from the OCT images were 2.25° ± 1.93° and 0.36 ± 0.19 mm, respectively. These findings are consistent with the findings of Oshika et al. (23).

There are several previous studies on the tilt and decentration of IOLs (24–30). Holladay et al. (31) reported that the degree of spherical aberration resulting from an IOL position anomaly was sufficient to decrease visual acuity when the decentration was more than 0.4 mm and the tilt was more than 7°. Tzelikis et al. (32) reported that decreases in ocular spherical aberration resulted in increased contrast sensitivity and visual acuity. Dietze and Cox (33) reported that increased intraocular lens decentration resulted in increased coma aberration.

Some patients (patients 17–24) were excluded from the statistical analysis in the present study due to unclear lens images in the anterior segment views. This may be because of the properties of their IOLs. The brands of these patients' IOLs were Dr. Schmidt (Dr. Schmidt intraocular linsen GmbH-Sankt Augustin, Germany) in 6 patients, Eye-O-Care (Eye-O-Care, Mumbai, India) in 1 patient,

and Eyekon (Eyekon, Florida, USA) in 1 patient. In the end, 32.5% of the patients were not measured. This is a weakness of OCT.

Anterior segment OCT has been shown to provide sensitive measurements but not in all cases. High-frequency ultrasonic and confocal microscopy provide image resolutions similar to that of OCT but OCT is more practical as it is a noncontact technology that provides both a wide image and a good evaluation field. One study has shown that anterior segment OCT depicted lens contours more clearly than Scheimpflug video photography (14).

In summary, there are many methods to evaluate the position of scleral-fixated IOLs. Each method has some advantages and some deficiencies. Our study is the first study to evaluate the position of scleral-fixated IOLs using anterior segment OCT. The positions of scleral-fixated IOLs can be evaluated highly accurately and objectively using anterior segment OCT. This technique has the advantages of being a noncontact, noninvasive, reproducible, and reliable method of evaluation. However, the number of patients in our study was limited. Further studies are warranted.

References

1. Baykara M, Ertürk H, Avcı R, Karataş A, Akova B. Skleral fiksasyon yöntemi ile göz içi lens implantasyonu. Turk J Ophthalmol 2004; 34: 55–60 (article in Turkish with summary in English).

2. Trimarchi F, Stringa M, Vellani G, Iato MS. Scleral fixation of an intraocular lens in the absence of capsular support. J Cataract Refract Surg 1997; 23: 795–797.

3. Bashshur Z, Ma'luf R, Najjar D, Noureddin B. Scleral fixation of posterior chamber intraocular lenses using fascia lata to cover the knots. Ophthalmic Surg Lasers 2002; 33: 445–449.

4. Kozaki J, Tanihara H, Yasuda A, Nagata M. Tilt and decentration of the implanted posterior chamber intraocular lens. J Cataract Refract Surg 1991; 17: 592–595.

5. Boyd BF, Agarwal A. Wavefront analysis and corneal topography. In: Boyd BF, Agarwal A, Alio JL, Krueger RR, Wilson SE, editors. Wavefront Analysis, Aberrometers and Corneal Topography. Panama; Highlights of Ophthalmology; 2003. pp. 217–242.

6. Özdamar A. Aberometreler ve topografi aracılı laser sistemleri. In: The 24th Turkish National Ophthalmology Training, Refractive Surgery; 2004. pp. 65–68.

7. Obstbaum SA, To K. Posterior chamber intraocular lens dislocations and malpositions. Aust N Z J Ophthalmol 1989; 17: 265–271.

8. Lyle WA, Jin JC. An analysis of intraocular lens exchange. Ophthalmic Surg 1992; 23: 453–458.

9. Auffarth GU, Wilcox M, Sims JC, McCabe C, Wesendahl TA, Apple DJ. Analysis of 100 explanted one-piece and three-piece silicone intraocular lenses. Ophthalmology 1995; 102: 1144–1150.

10. Carlson AN, Stewart WC, Tso PC. Intraocular lens complications requiring removal or exchange. Surv Ophthalmol 1998; 42: 417–440.

11. Mamalis N, Davis B, Nilson CD, Hickman MS, Leboyer RM. Complications of foldable intraocular lenses requiring explantation or secondary intervention – 2003 survey update. J Cataract Refract Surg 2004; 30: 2209–2218.

12. Chakrabarti A, Gandhi RK, Chakrabarti M. Ab externo 4-point scleral fixation of posterior chamber intraocular lenses. J Cataract Refract Surg 1999; 25: 420–426.

13. Duffey RJ, Holland EJ, Agapitos PJ, Lindstrom RL. Anatomic study of transsclerally sutured intraocular lens implantation. Am J Ophthalmol 1989; 108: 300–309.

14. Steinert RF, Huang D. Anterior Segment Optical Coherence Tomography. Thorofare, NJ, USA: SLACK Inc.; 2008.

15. Kozaki J, Takahashi F. Theoretical analysis of image defocus with intraocular lens decentration. J Cataract Refract Surg 1995; 21: 552–555.

16. Steiner A, Steinhorst UH, Steiner M, Theischen M, Winter R. [Ultrasound biomicroscopy for localization of artificial lens haptics after transscleral suture fixation]. Ophthalmologe 1997; 94: 41–44.

17. Holland EJ, Djalilian AR, Pederson J. Gonioscopic evaluation of haptic position in transsclerally sutured posterior chamber lenses. Am J Ophthalmol 1997; 123: 411–413.

18. Durak A, Oner HF, Koçak N, Kaynak S. Tilt and decentration after primary and secondary transsclerally sutured posterior chamber intraocular lens implantation. J Cataract Refract Surg 2001; 27: 227–232.

19. Sasaki K, Sakamoto Y, Shibata T, Nakaizumi H, Emori Y. Measurement of postoperative intraocular lens tilting and decentration using Scheimpflug images. J Cataract Refract Surg 1989; 15: 454–457.

20. Teichmann KD, Teichmann IA. The torque and tilt gamble. J Cataract Refract Surg 1997; 23: 413–418.

21. Lubniewski AJ, Holland EJ, Van Meter WS, Gussler D, Parelman J, Smith ME. Histologic study of eyes with transsclerally sutured posterior chamber intraocular lenses. Am J Ophthalmol 1990; 110: 237–243.

22. Hayashi K, Hayashi H, Nakao F, Hayashi F. Intraocular lens tilt and decentration, anterior chamber depth, and refractive error after trans-scleral suture fixation surgery. Ophthalmology 1999; 106: 878–882.

23. Oshika T, Sugita G, Miyata K, Tokunaga T, Samejima T, Okamoto C, Ishii Y. Influence of tilt and decentration of scleral-sutured intraocular lens on ocular higher-order wavefront aberration. Br J Ophthalmol 2007; 91:185–188.

24. Auran JD, Koester CJ, Donn A. In vivo measurement of posterior chamber intraocular lens decentration and tilt. Arch Ophthalmol 1990; 10: 875–879.

25. Hayashi K, Hayashi H, Nakao F, Hayashi F. Intraocular lens tilt and decentration after implantation in eyes with glaucoma. J Cataract Refract Surg 1999; 25: 1515–1520.

26. Hayashi K, Hayashi H, Nakao F, Hayashi F. Anterior capsule contraction and intraocular lens decentration and tilt after hydrogel lens implantation. Br J Ophthalmol 2001; 85: 1294–1297.

27. Kim JS, Shyn KH. Biometry of 3 types of intraocular lenses using Scheimpflug photography. J Cataract Refract Surg 2001; 27: 533–536.

28. Nejima R, Miyata K, Honbou M, Tokunaga T, Tanabe T, Sato M, Oshika T. A prospective, randomised comparison of single and three piece acrylic foldable intraocular lenses. Br J Ophthalmol 2004; 88: 746–749.

29. Taketani F, Matuura T, Yukawa E, Hara Y. Influence of intraocular lens tilt and decentration on wavefront aberrations. J Cataract Refract Surg 2004; 30: 2158–2162.

30. Baumeister M, Neidhardt B, Strobel J, Kohnen T. Tilt and decentration of three-piece foldable high-refractive silicone and hydrophobic acrylic intraocular lenses with 6-mm optics in an intraindividual comparison. Am J Ophthalmol 2005; 140: 1051–1058.

31. Holladay JT, Piers PA, Koranyi G, van der Mooren M, Norrby NE. A new intraocular lens design to reduce spherical aberration of pseudophakic eyes. J Refract Surg 2002; 18: 683–691.

32. Tzelikis PF, Akaishi L, Trindade FC, Boteon JE. Spherical aberration and contrast sensitivity in eyes implanted with aspheric and spherical intraocular lenses: a comparative study. Am J Ophthalmol 2008; 145: 827–833.

33. Dietze HH, Cox MJ. Limitations of correcting spherical aberration with aspheric intraocular lenses. J Refract Surg 2005; 21: 541–546.